The Journal of Experimental Biology 205, 189–200 (2002)
Printed in Great Britain © The Company of Biologists Limited 2002
JEB3734



# Effects of longitudinal body position and swimming speed on mechanical power of deep red muscle from skipjack tuna (*Katsuwonus pelamis*)

Douglas A. Syme[1,*] and Robert E. Shadwick[2]

[1]*Department of Biological Sciences, University of Calgary, 2500 University Drive NW, Calgary, Alberta, Canada T2N 1N4* and [2]*Marine Biology Research Division, Scripps Institution of Oceanography, University of California, San Diego, La Jolla, CA 92093-0204, USA*

*e-mail: syme@ucalgary.ca

*Accepted 31 October 2001*

## Summary

**The mechanical power output of deep, red muscle from skipjack tuna (*Katsuwonus pelamis*) was studied to investigate (i) whether this muscle generates maximum power during cruise swimming, (ii) how the differences in strain experienced by red muscle at different axial body locations affect its performance and (iii) how swimming speed affects muscle work and power output. Red muscle was isolated from approximately mid-way through the deep wedge that lies next to the backbone; anterior (0.44 fork lengths, ANT) and posterior (0.70 fork lengths, POST) samples were studied. Work and power were measured at 25 °C using the work loop technique. Stimulus phases and durations and muscle strains (±5.5 % in ANT and ±8 % in POST locations) experienced during cruise swimming at different speeds were obtained from previous studies and used during work loop recordings. In addition, stimulus conditions that maximized work were determined. The stimulus durations and phases yielding maximum work decreased with increasing cycle frequency (analogous to tail-beat frequency), were the same at both axial locations and were almost identical to those used by the fish during swimming, indicating that the muscle produces near-maximal work under most conditions in swimming fish. While muscle in the posterior region undergoes larger strain and thus produces more mass-specific power than muscle in the anterior region, when the longitudinal distribution of red muscle mass is considered, the anterior muscles appear to contribute approximately 40 % more total power. Mechanical work per length cycle was maximal at a cycle frequency of 2–3 Hz, dropping to near zero at 15 Hz and by 20–50 % at 1 Hz. Mechanical power was maximal at a cycle frequency of 5 Hz, dropping to near zero at 15 Hz. These fish typically cruise with tail-beat frequencies of 2.8–5.2 Hz, frequencies at which power from cyclic contractions of deep red muscles was 75–100 % maximal. At any given frequency over this range, power using stimulation conditions recorded from swimming fish averaged 93.4±1.65 % at ANT locations and 88.6±2.08 % at POST locations (means ± S.E.M., *N*=3–6) of the maximum using optimized conditions. When cycle frequency was held constant (4 Hz) and strain amplitude was increased, work and power increased similarly in muscles from both sample sites; work and power increased 2.5-fold when strain was elevated from ±2 to ±5.5 %, but increased by only approximately 12 % when strain was raised further from ±5.5 to ±8 %. Taken together, these data suggest that red muscle fibres along the entire body are used in a similar fashion to produce near-maximal mechanical power for propulsion during normal cruise swimming. Modelling suggests that the tail-beat frequency at which power is maximal (5 Hz) is very close to that used at the predicted maximum aerobic swimming speed (5.8 Hz) in these fish.**

Key words: mechanical power, red muscle, swimming speed, tail-beat frequency, strain, work loop, isometric twitch, skipjack tuna, *Katsuwonus pelamis*, stimulation.

## Introduction

Muscles used in locomotion are known to have a variety of functions (Biewener and Gillis, 1999), including powering propulsion (e.g. Biewener, 1998; Rome et al., 1993; Stevenson and Josephson, 1990), braking and stability (Full et al., 1998) or acting as struts to transmit energy to/from elastic elements or the limbs (Roberts et al., 1997; Biewener et al., 1998). It is therefore not surprising that muscles used during steady locomotion may not be recruited in a way that simply maximizes power production. The trunk muscles of some fish show regional specializations in contraction kinetics (e.g. Rome et al., 1993; Altringham et al., 1993; Davies and Johnston, 1993; Altringham and Block, 1997; Wardle et al., 1989; Coughlin, 2000), and there are well-documented changes in strain and its phase, and in the duration of electromyographic activity and its phase, along the length of fish (Franklin and Johnston, 1997; Hammond et al., 1998;

Coughlin, 2000) (for a review, see Shadwick et al., 1998). Such regional differences in activation and strain along the length of the fish reflect differences in muscle function; some fish generate the bulk of work anteriorly, others posteriorly, and some appear to use posterior muscle to transmit energy at the expense of power production (Wardle et al., 1995; Shadwick et al., 1998; Altringham and Ellerby, 1999) (for references, see Coughlin, 2000). Although all red trunk musculature (i.e. that used for steady swimming) studied thus far serves a power-producing role, the absence of examples demonstrating that this is its sole function suggests that most fish are not designed to maximize cruising speed.

Tuna, like other fish, use their red muscles to power steady, cruise swimming and only recruit their white muscle to power rapid bursts (Rayner and Keenan, 1967; Knower et al., 1999). However, the exceedingly high oxidative capacity of tuna red muscle probably allows it to power sustained speeds that are higher than in other fish (Johnston and Tota, 1974). Tuna are thus considered to be high-performance cruise swimmers (George and Stevens, 1978), which require high levels of power from their red muscle. Tuna also have a particularly derived anatomy in which the bulk of the oxidative (red) muscle is located midway between the head and tail, but its cyclic contractions are directed posteriorly to the caudal fin. The limited bending in regions of the body where the red muscle resides, and the fact that undulations of the trunk are not required to transmit force to the water in thunniform swimming, could imply that much of the red muscle mass of a tuna acts largely as a strut to transmit force to the tail. Equally intriguing, the limited bending at any point on the fish where there are significant amounts of red muscle and the considerable proportion of red muscle that resides medially where strain could be further limited by the close proximity to the neutral axis of bending could, in fact, limit its ability to do work. Thus, it is possible that very little work and power could be produced by these muscles in the first place.

However, recent evidence shows that the activation patterns in tuna red muscle are consistent with those used to produce work (Shadwick et al., 1999; Altringham and Block, 1997). Further, the strains in the superficial and deep red muscles are substantially out of phase with one another, indicating that these fish have been freed from the constraints of limited muscle shortening during limited body bending by having deep red muscle that is able to shorten independently of the surrounding tissue (Shadwick et al., 1999; Katz et al., 2001). Thus, given these kinematics and the requirement to power high-speed swimming, it seems almost certain that the deep red muscle is designed to produce mechanical power to generate thrust at the tail and that it can produce substantial amounts of power. The presence of robust tendons linking myotomal muscle to the vertebrae and caudal fin supports this view.

To test the hypothesis that the sole mechanical function of the deep red muscle of skipjack tuna *Katsuwonus pelamis* is to produce power for locomotion, we measured the work- and power-generating capacity of muscle isolated from the fish when experiencing the same strain (shortening) and stimulus conditions (phase and duration) as during swimming, and compared these values with the maximum of which the muscle is capable. Recordings were made from muscle at anterior and posterior locations to determine how the different strains and stimulus conditions experienced at these two locations affect performance and whether muscle from both locations has the same ultimate function. We also measured work and power over a range of cycle frequencies (tail-beat frequencies) to determine whether the frequencies used by cruising fish are, in fact, those that yield maximal power from these muscles and also as a step towards understanding how much power the red muscles are capable of producing in relation to what is required to swim at different speeds. As there are no direct measures of the mechanical power output required for swimming in these fish and little is known about the power output of tuna red muscle *in vivo* [see Altringham and Block (1997) for an estimate], we have only a limited understanding of how much of the red muscle mass is required to generate the requisite power to swim at the high speeds observed in these fish. Such estimates will allow us to understand better the function and potential of tuna red muscle.

## Materials and methods

Studies were conducted at the National Marine Fisheries Service, Kewalo Research Facility in Honolulu, Hawaii. Skipjack tuna (*Katsuwonus pelamis* L.), 36–45.5 cm in body length, were caught on barbless hooks by local commercial fisherman and then transferred to 7 m diameter, 1 m deep holding tanks. The tanks had a continuous supply of fresh sea water (at approximately 25 °C) and aeration. Fish were fed daily with chopped squid and fish until satiation. Fish were held for 1 day to a week before experiments and were feeding and appeared healthy. All care and experimental procedures were carried out according to protocols approved by the University of California.

### *Muscle preparation*

Fish were captured with a dip net and immediately killed with a blow to the head followed by severing the spinal cord. A fillet of muscle was quickly cut from the side of the fish, extending from near the caudal peduncle to the head and laterally approximately midway through the interior wedge of red muscle. Red muscle was removed from the interior, deep wedge at a posterior (POST) location (0.69–0.72 fork lengths, mean 0.70 fork lengths) and an anterior (ANT) location (0.42–0.46 fork lengths, mean 0.44 fork lengths) (Fig. 1). These blocks of muscle, 2–5 myotomes long, were then pared down to a single myotome with a bundle of fibres approximately 0.5 mm in diameter remaining and strips of myosepta at each end. Dissections were performed at 5–10 °C. The muscle was rinsed frequently with chilled saline, modified from Altringham and Block (1997), during dissections (composition, in mmol $l^{-1}$: NaCl, 175.5; KCl, 2.6; $CaCl_2$, 2.7; $MgCl_2$, 1.1; sodium pyruvate, 10; Hepes, 10; pH 7.8 at 25 °C, saturated with pure oxygen). Muscles were then transferred to

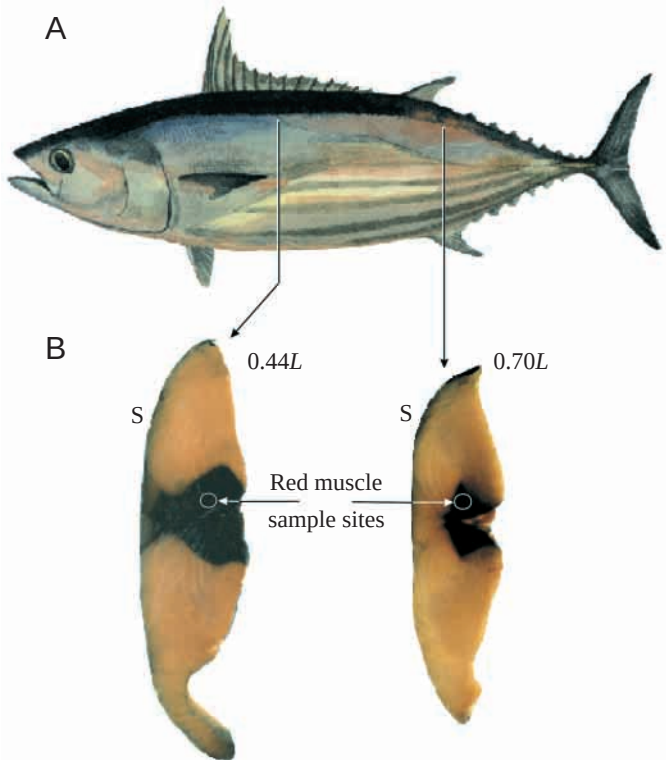


Fig. 1. (A) Lateral view of a skipjack tuna (adapted from Joseph et al., 1988) showing the position of anterior (0.44*L*) and posterior (0.70*L*) muscle sample sites. *L*, fork body length. (B) Hemi-transverse sections of the body showing the location of the deep red muscle. S, skin.

an experimental chamber filled with circulating saline at 25 °C and bubbled with pure oxygen. The myoseptum at one end was tied to a stainless-steel pin connected to a servomotor arm (model 350, Cambridge Technology, MA, USA) and at the other end to a pin connected to a force transducer (AE801; SensoNor, Horten, Norway). The preparation was stretched to remove visible slack. A platinum-tipped stimulating electrode was positioned next to the muscle, and stimulus voltage was increased until a maximal isometric twitch was elicited (4 ms pulse duration). A clearly defined peak in the length/twitch-force relationship was not evident, so a combination of isometric force and work recordings was used to determine the optimal length; muscle length was adjusted so that developed twitch force and work were near-maximal and passive tension during work recordings was not excessive. A stimulus frequency of 40 Hz was found to give maximal tetanic force and was used during all subsequent measurements of force and work.

### *Work and power recordings*

Mechanical work and power were determined using the work loop method (Josephson, 1985, 1993). Briefly, a servomotor subjected the muscle to sinusoidal length changes (strain) centred about the optimal length; a sinusoidal strain trajectory is a very good approximation of the actual strain trajectory of the red muscle in scombrid fish [Pacific bonito *Sarda chilienesis* (Ellerby et al., 2000); skipjack tuna (Shadwick et al., 1999)]. Strain amplitude is expressed as a percentage of the resting length. The muscle was stimulated phasically during the strain cycle such that force was developed primarily during muscle shortening and the muscle was relaxed during lengthening. Stimulus phase is the point during the strain cycle that the stimulus began and is expressed in degrees of the sine cycle, with 0 ° representing the initial length, 90 ° the maximum length and 270 ° the minimum length. Work and power were measured over a range of cycle frequencies, strain amplitudes and stimulus durations and phases that encompassed the physiological conditions measured from swimming skipjack tuna of similar size; swimming data were from Shadwick et al. (1999) and Knower et al. (1999). These included cycle frequencies of 1–15 Hz and ±5.5 % strain for ANT muscle and ±8 % strain for POST muscle. At each cycle frequency and strain combination, stimulus duration and phase were systematically altered until the net work produced by the muscle was maximized; in all cases, the physiological values were included in the series tested. The muscle was subjected to three cycles of strain and stimulation at each combination; measurements were taken from the second or third cycle. Work was calculated as the integral of force with respect to muscle length over the complete sinusoidal strain cycle. Power is the rate of doing work and equals the product of work per cycle and cycle frequency. Isometric tetanic force was recorded routinely throughout the experiments. If force changed from the initial level, subsequent work values were adjusted assuming a linear change in force and work between recordings.

Work and power are expressed as a percentage of the maximum for each preparation. Because of the very small size of the preparations, their irregular dimensions and uncertainties about the viability of the entire bundle, we did not attempt either to weigh them or to measure their volume. To calculate absolute power, which is required to estimate the maximum swimming speed, muscle mass was estimated as follows at the conclusion of the experiment, which normally lasted 3–5 h. The length of the muscle fibres within the bundles was measured under a microscope; the fibres were parallel in all cases. Muscle cross-sectional area was estimated using measured isometric force and assuming that each preparation generated 140 kN m$^{-2}$ maximal isometric tetanic stress. Muscle mass was then calculated assuming a density of 1050 kg m$^{-3}$. The value of 140 kN m$^{-2}$ was chosen on the basis of the following. Fast-twitch muscle fibres generate approximately 200–300 kN m$^{-2}$ maximal, isometric, tetanic stress (e.g. Langfeld et al., 1989; Altringham and Johnston, 1988; Bottinelli et al., 1991; Close, 1972; Eddinger, 1998); we chose 250 kN m$^{-2}$ as an intermediate estimate. Fast-twitch fibres have a myofibril volume density of approximately 95 % (e.g. Sieck et al., 1998), and skipjack deep red fibres have a myofibril volume density of 66 % (Mathieu-Costello et al., 1992), so individual tuna red fibres will generate approximately 175 kN m$^{-2}$. After accounting for extracellular space and connective tissue, we estimate the fibre volume density of skipjack red muscle bundles to be 80 % on the basis

of fibre volume densities of 69 % in scup (*Stenotomus chrysops*) red muscle (Zhang et al., 1996), 69 % in trout (*Oncorhynchus mykiss*) red muscle (D. J. Coughlin, personal commmunication) and 57 % in carp (*Cyprinus carpio*) red muscle (Rome and Sosnicki, 1990) and an estimate of 88 % in tuna red muscle (O. Mathieu-Costello, personal commmunication). Given a fibre volume density of 80 % and a fibre stress of 175 kN m$^{-2}$, whole tuna red muscle will then generate approximately 140 kN m$^{-2}$. This compares with 125–130 kN m$^{-2}$ for trout, bass (*Micropterus salmoides*) and scup (Coughlin, 2000; Rome et al., 1992) red muscle based on fibre volume densities of 0.69 as indicated above, and 140 kN m$^{-2}$ for trout red muscle bundles reported by Hammond et al. (1998).

Values are reported as mean ± standard error (S.E.M.); $N$=3 or 4 for ANT and $N$=5 or 6 for POST. Comparisons were made using analyses of variance (ANOVAs) and Tukey's tests or $t$-tests where appropriate. A 5 % level of significance was used in all cases.

## Results

### *Work and power*

The values of work and power reported in this study are net work and power, which is calculated over a complete length cycle. Because any work done to stretch the muscle must come at the expense of work done by contralateral muscles, net work best represents the energy the muscle contributes to propulsion during a tail-beat cycle. Absolute values of work (J kg$^{-1}$) and power (W kg$^{-1}$) are reported on the basis of the above assumptions about muscle stress.

Work loops generated by muscle from ANT and POST locations at different cycle frequencies and stimulus conditions are shown in Fig. 2. The loops generated using stimulus conditions measured from swimming fish are strikingly similar to those generated using stimulus conditions that maximize work. Using optimized stimulus conditions, muscle from both ANT and POST locations produced maximum work per cycle at cycle frequencies of 2–3 Hz (Fig. 3) (ANT=12.4±1.42 J kg$^{-1}$ at ±5.5 % strain; POST=19.8±1.89 J kg$^{-1}$ at ±8 % strain). Work declined to near zero at 15 Hz, the highest frequency tested, and also declined as the frequency decreased below 2 Hz (Fig. 3). Using optimized stimulus conditions, power output was maximal at a cycle frequency of 4–5 Hz in the ANT location and 5 Hz in the POST location (Fig. 4) (ANT=44.4±9.97 W kg$^{-1}$ at ±5.5 % strain; POST=74.9±10.4 W kg$^{-1}$ at ±8 % strain). Power dropped rapidly as frequency increased or decreased from the optimal value. At any given cycle frequency, the work and power produced by the muscle when activated using the phases and stimulus durations measured from swimming fish were the same as or only slightly less (85–100 %) than the maximum that could be produced by the muscle when both phase and strain were optimized (Figs 2–4), except at the slowest frequency in POST muscle, at which work under *in vivo* conditions was notably reduced.

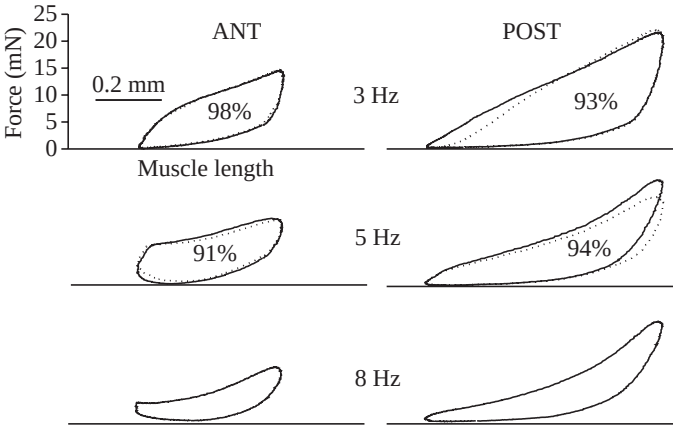


Fig. 2. Work loops from internal red muscle of a skipjack tuna. Results from two different longitudinal body locations and three different cycle frequencies are shown. Muscle length was cycled in a sinusoidal fashion, and the muscle was stimulated phasically during the length cycle. Loops are plots of muscle force against length for a complete length cycle and are traversed in a counterclockwise direction. Net work is equal to the area inside the loop. Left-hand panels: muscle from an anterior (ANT) location (0.45$L$); resting length 4.0 mm, strain ±5.5 %. Right-hand panels: muscle from a posterior (POST) location (0.69$L$); resting length 4.5 mm, strain ±8 %. Both muscles are from the same fish. Work loops generated using stimulus parameters that maximized work output (solid lines) are shown together with loops generated when the muscle was stimulated using parameters measured from swimming fish (broken lines). Values inside loops are the net work done using stimulus parameters from swimming fish (broken loops) as a percentage of the maximum (solid loops). Note the similarity between the two types of loop. Only maximal loops are shown at 8 Hz because fish do not normally swim at this speed using only red muscle.

At a constant cycle frequency (4 Hz), power increased with increasing strain up to the largest strain recorded from red muscle in swimming skipjack (Fig. 5). The relationship with strain was not linear. Power increased in approximate proportion to strain between ±2 % and ±5.5 % strain (a 2.5-fold increase in power with a 2.75-fold increase in strain, $P$<0.05). However, when strain was increased further from ±5.5 % to ±8 %, the increase in power was smaller and less than proportional (a 1.12-fold increase in power with a 1.45-fold increase in strain, $P$<0.05). While strains larger than ±8 % were not tested (nor were they observed in swimming fish), in muscles from both locations there was clear evidence of power reaching a plateau in this strain range. There was no significant difference in the relative power produced by muscle from the two locations when compared at the same strain amplitude (Fig. 5, $P$=0.57).

### *Activation parameters:* in vivo *and optimal*

At all frequencies studied, the stimulus phases resulting in maximal work (optimal phase) were between 0 and 90 ° (Fig. 6), meaning that stimulation began while the muscle was still being lengthened, thus enhancing force production. The optimal stimulus phase decreased with increasing cycle

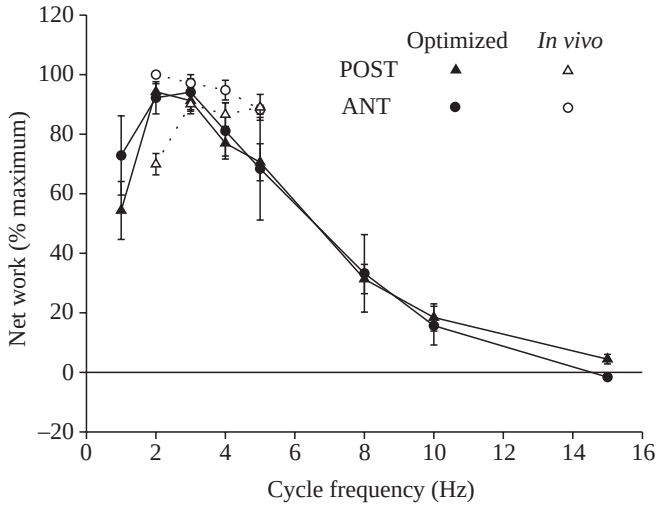


Fig. 3. Net work per cycle as a function of cycle frequency (tail-beat frequency) from internal red muscle of skipjack tuna at anterior (ANT) and posterior (POST) locations. Filled symbols and solid lines show results using optimized stimulus conditions that maximize work (optimized) and are expressed as a percentage of the largest value recorded over the range of frequencies studied. Open symbols and broken lines are work done when the muscle was stimulated using conditions measured from swimming fish (*in vivo*) and are expressed as a percentage of the maximum (optimized) value at each of the frequencies indicated; they therefore show the performance of the muscle under *in vivo* conditions relative to the maximum (optimized) of which the muscle is capable at each frequency. The limited range of frequencies covered using *in vivo* conditions reflects the range over which fish actually swim using only red muscle. The strain for ANT muscle was ±5.5 % and that for POST muscle was ±8 %, reflecting strains used *in vivo*. Values are means ± S.E.M., *N*=3–6.

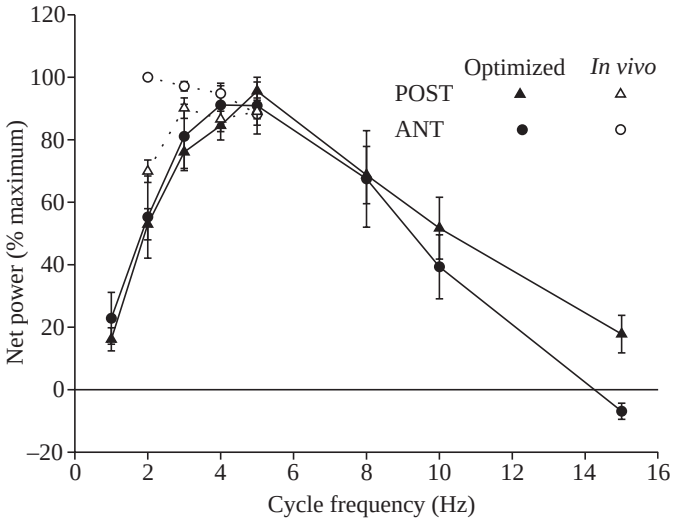


Fig. 4. Net power output as a function of cycle frequency (tail-beat frequency). See legend to Fig. 3 for further details. Values are means ± S.E.M., *N*=3–6.

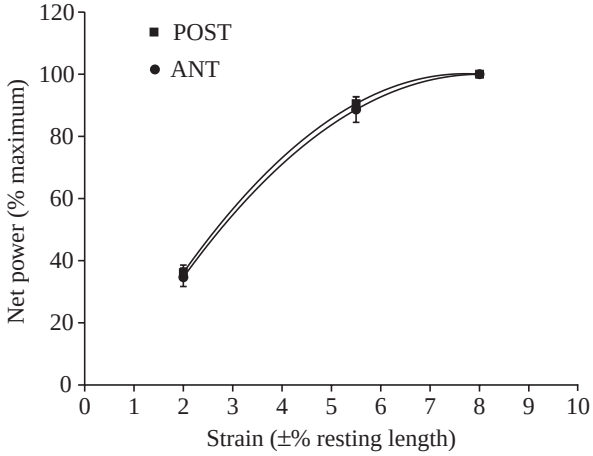


Fig. 5. Net power output as a function of strain amplitude from internal red muscle of skipjack tuna at anterior (ANT) and posterior (POST) locations. Strain is the peak amplitude of the imposed length cycle as a percentage of muscle length. The cycle frequency was 4 Hz in all cases. Power is expressed as a percentage of the value at 8 % strain. The muscle was stimulated using conditions measured from swimming fish. Higher strains result in significantly higher power outputs (two-way ANOVA and Tukey's test, $P<0.05$). Values are means ± S.E.M., *N*=3–6.

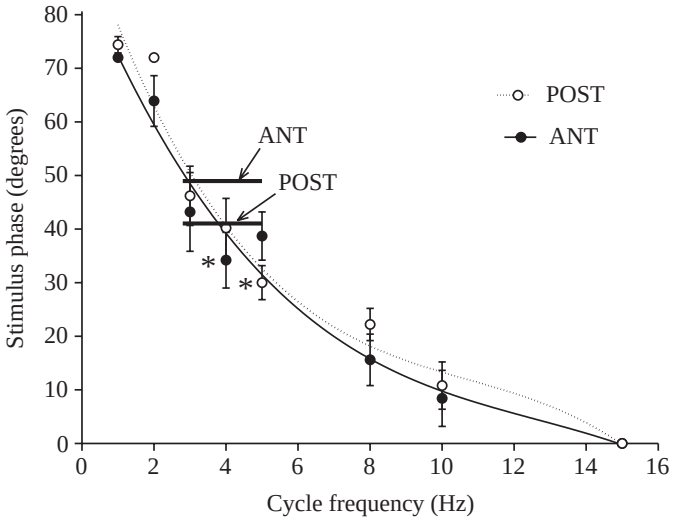


Fig. 6. Stimulus phase as a function of cycle frequency. Phase is the time of stimulus onset during the sinusoidal length cycle, in degrees, where 0 ° is muscle lengthening through resting length and 90 ° is maximum muscle length just prior to shortening. Data from anterior (ANT) and posterior (POST) locations are shown. Curves show the optimal stimulus phases required to maximize net work output from isolated muscle. Heavy bars show the stimulus phases used by swimming fish (Shadwick et al., 1999). Asterisks indicate optimal phases that are significantly different ($P<0.05$) from those used *in vivo*. The limited range of phases from swimming fish reflects the limited range over which fish actually swim using only red muscle. Values are means ± S.E.M., *N*=3–6.

frequency, reaching 0 ° at a cycle frequency of 15 Hz (i.e. the muscle was stimulated in the middle of its lengthening trajectory). At any given frequency, the optimal phases were the same in muscles from both longitudinal body locations and were very similar to the onset phases of electromyographic (EMG) activity used by swimming skipjack (Fig. 6, heavy bars

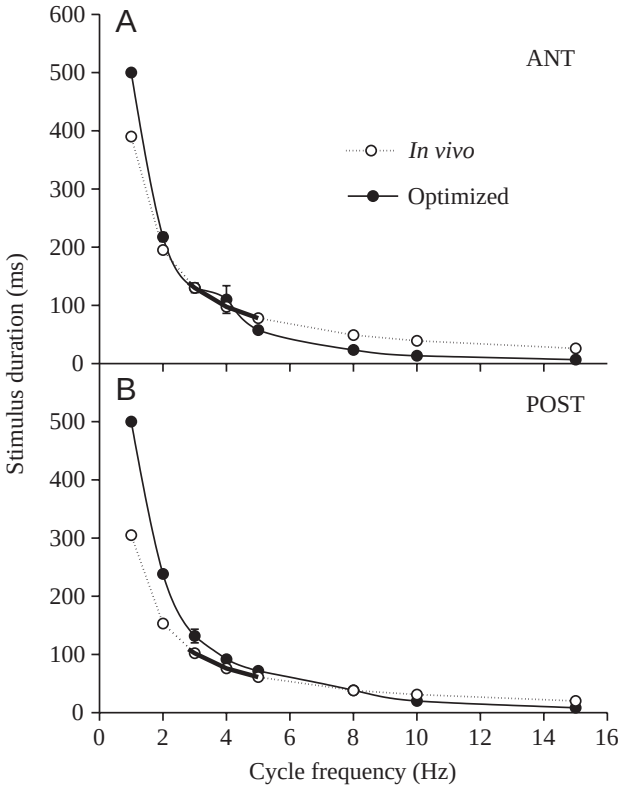


Fig. 7. Stimulus duration as a function of cycle frequency. (A) Data from anterior (ANT) locations; (B) data from posterior (POST) locations. Filled lines and solid symbols show optimal stimulus durations required to maximize net work output from isolated muscle (optimized). Dotted lines and open symbols show stimulus durations used by swimming fish (*in vivo*) (Shadwick et al., 1999); the heavy portions highlight speeds at which fish actually swim using only red muscle; the remainder of the *in vivo* curve is an extrapolation from these data. Values are means ± S.E.M., $N$=3–6.

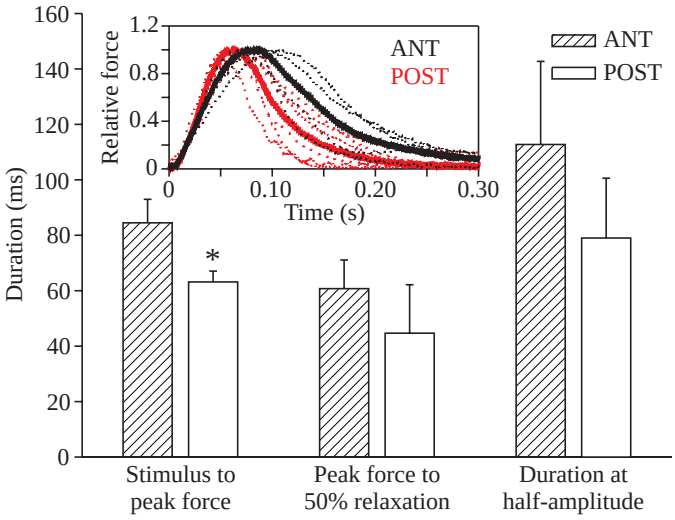


Fig. 8. Isometric twitch kinetics of internal red muscle from anterior (ANT) and posterior (POST) locations at 25 °C. 'Stimulus to peak force' is the time from the stimulus until the peak of the twitch. 'Peak force to 50 % relaxation' is the time from the peak of the twitch until developed force declined to 50 % maximal. 'Duration at half-amplitude' is the period over which force remained 50 % maximal or greater. An asterisk indicates a significant difference ($P$<0.05) between locations. Values are means + S.E.M., $N$=4–6. The inset shows isometric twitches of internal red muscle from anterior (ANT, black) and posterior (POST, red) locations at 25 °C. Fine broken lines are twitches from individual preparations; heavy solid lines are composite twitches made by scaling recordings from individual preparations and then averaging the data sets.

compared with curves). In ANT muscle, the optimal phases were not significantly different from the phases used by swimming fish at 3 and 5 Hz ($P$=0.46 at 3 Hz; $P$=0.06 at 5 Hz), but were marginally lower at 4 Hz ($P$=0.03). In POST muscle, the optimal phases were not significantly different from the phases used by swimming fish at 3 and 4 Hz ($P$=0.37 at 3 Hz; $P$=0.88 at 4 Hz), but were lower at 5 Hz ($P$=0.006).

The stimulus duration required to maximize work (optimal duration) decreased with increasing cycle frequency (Fig. 7). The optimal stimulus durations were the same as or less than the duration of the shortening portion of the length cycle (half the cycle period). Over the range of tail-beat frequencies at which fish were observed to swim using only red muscle (2.8–5.2 Hz) (Knower et al., 1999), the EMG burst durations and optimal stimulus durations matched very well (Fig. 7, heavy bars compared with solid curves). Even when the EMG durations were extrapolated to tail-beat frequencies well outside the range used by cruising fish, there remained a good match between predicted EMG burst duration and optimal stimulus duration (Fig. 7, solid compared with dotted curves), except at very slow frequencies.

### *Twitch parameters*

Twitches from ANT muscle were slower in time from stimulus to peak force than twitches from POST muscle ($P$=0.033), were not significantly different in relaxation rate (peak force to 50 % relaxation, $P$=0.22) and only approached being significantly longer in duration at half-amplitude ($P$=0.070) (Fig. 8). The absolute difference in time to peak force was approximately 21 ms longer in ANT muscle, which corresponds to a 33 % slower rise time compared with POST muscle. To appreciate better the differences and variability, isometric twitches from muscles at both locations were scaled and then averaged (Fig. 8 inset). In addition to a longer time to peak force, the ANT muscles also appear to have a more prolonged twitch duration as a result of very slow relaxation during the later stages of the twitch.

### *Instantaneous power in simulated swimming*

To simulate the temporal relationship of muscle power production along the body of a swimming skipjack, we calculated instantaneous power as a function of time, as in Altringham et al. (1993) from work loop force and length recordings at 3–5 Hz. Fig. 9 shows an example of this from one fish for muscle at 0.42$L$ (ANT) and 0.70$L$ (POST), where $L$ is fork length, at a cycle frequency of 4 Hz. Results from other fish and at other frequencies were very similar. Relative to the

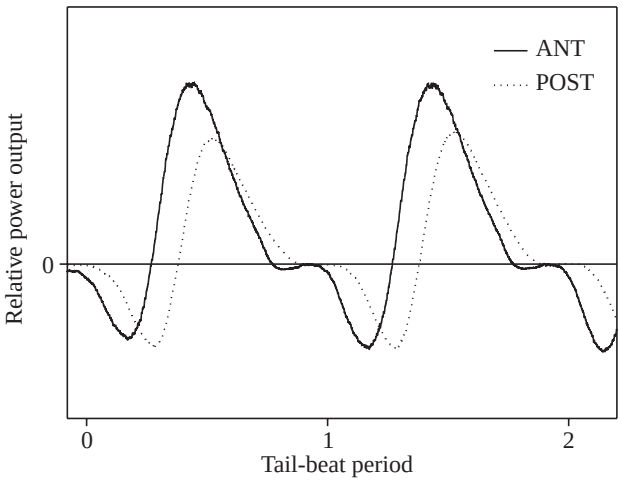


Fig. 9. Simulation of relative power output of red muscle from anterior (ANT) (0.42*L*) and posterior (POST) (0.70*L*) locations in a 43 cm skipjack tuna during cyclic contractions at 4 Hz (the tail-beat frequency for steady swimming at approximately $3\,L\,s^{-1}$). *L*, fork body length. Plots show instantaneous power *versus* time (see Altringham et al., 1993), where power (i.e. force × shortening velocity) was calculated from work loop data; velocity is the time derivative of the length trace, with positive velocity occurring during shortening. The traces for POST muscle have been delayed by 40 ° to show the proper temporal relationship between the two locations. The amplitudes of ANT and POST power curves are scaled to account for the differences in cross-sectional area of red muscle and mass-specific power output at these locations (see text for details).

anterior power curves, the posterior curves have been delayed in time by 40 °, or 0.112 cycle periods, based on the estimation that the muscle shortening wave travels along the body of a swimming skipjack at approximately $2.5\,L$ cycle period$^{-1}$ (Shadwick et al., 1999). By doing this, we show the time course of power production at the two locations as it would occur in a swimming fish. The power curves for muscle in the ANT and POST locations have the same shape, with a predominantly positive component. The high strain wave speed results in near-synchrony in power production all along the internal red muscle loin (i.e. the muscles at these two locations attain peak power outputs within approximately 10 % of a cycle of one another). Because muscle strain increases posteriorly, mass-specific net work and power production are greater in POST than in ANT locations. However, when mass-specific power is scaled to account for the 2.4-fold greater cross-sectional area of red fibres at 0.42*L* compared with 0.7*L* (Knower et al., 1999), the total power contribution from ANT locations is approximately 40 % greater than from POST locations.

## Discussion

### *Maximal work and power*

The finding that deep red muscle from both ANT and POST locations produced near-maximal work and power when activated under the conditions measured in swimming fish (Figs 2–7) provides strong support for the hypothesis that the sole function of the internal aerobic muscle is to maximize net mechanical power. Coughlin (2000) also compared maximal work in trout red muscle with that measured using *in vivo* activation parameters and found that, while the muscles produce substantial amounts of positive net work, muscle from ANT and POST locations produced only 24 % and 40 %, respectively, of the maximum of which they were capable. This mismatch suggests that fish such as trout do not attempt to maximize cruise swimming speed or that there are limitations preventing them from doing so. Hammond et al. (1998) found, also in rainbow trout red muscle, that the power output measured using *in vivo* stimulation was not always maximal; at cycle frequencies equal to and less than those giving peak power, power was close to maximal in muscle from posterior locations (0.5 and 0.65 total body lengths), but at anterior locations (0.35 body lengths) or at higher frequencies at all locations it was only approximately 60 % maximal. Rome and Swank (1992) found that red muscle in scup produced 87–98 % of maximum power at 20 °C when stimulated using strains and duty cycles measured from swimming fish (although stimulus phase was optimized in these experiments), but at 10 °C less than 20 % of maximum power was produced *in vivo*. Tuna, thus far, appear to show the highest priority for attaining maximum power from their muscles at all body locations and all cruise swimming speeds.

In tuna, thrust is generated primarily at the tail. On the basis of the relative cross-sectional distribution of red muscle in skipkack tuna (Knower et al., 1999; Graham et al., 1983) and the power produced by muscle from anterior and posterior locations (Fig. 4), we estimate that there is a significant contribution to power along the entire length of the fish, but considerably more (40 %) comes from anterior regions (see Results). If this power is transmitted to the tail through tendons (in parallel) and not other muscles (in series), then the longitudinal source and regional variations in absolute power output are not critical. Further, there is near-synchronous power production along the length of these fish (Fig. 9). While synchronous power production and localized muscle would be ineffectual at generating a propagated wave for carangiform swimming, it is very effective at generating maximum thrust at the tail in thunniform swimmers. In this way, all the muscle along the length of the fish contributes at once to powering the tail beat.

The thunniform mode of locomotion is possible in part because the deep, red fibres in tunas are connected to the axial skeleton *via* long tendons (Westneat et al., 1993). Therefore, contractile work generated in more anterior segments of muscle can be transmitted to the tail *via* tendons rather than through other muscles, allowing even the posterior-most muscle fibres to make a maximal contribution to thrust power. While other fish show an anterior-to-posterior increase in the ‘negative’ power component of the cycle (Wardle et al., 1995; Hammond et al., 1998), the tuna did not (Figs 4, 9), again suggesting that muscle along the entire length of the fish serves only to generate thrust power. These fish appear to be extracting all the power they can from their muscles to swim.

The estimated maximum power produced by skipjack tuna red muscles at a strain of ±5.5 % was approximately 40 W kg$^{-1}$. This is three times higher than that reported for red muscle in yellowfin tuna (*Thunnus albacares*) (12 W kg$^{-1}$ at ±5 % strain and 25 °C) (Altringham and Block, 1997) after accounting for the small difference in strain amplitude. However, after correcting for temperature ($Q_{10}$=2) and small differences in strain, our estimate is very close to that reported by Hammond et al. (1998) for whole trout red muscle (17 W kg$^{-1}$ at 9 °C and ±5 % strain) and by Coughlin (2000) for trout (11 W kg$^{-1}$ at 10 °C and approximately ±4.5 % strain) and bass (25 W kg$^{-1}$ at 20 °C and approximately ±5 % strain) red muscle fibres after accounting for an approximately 69 % fibre volume density. A likely reason for the discrepancy between our measurements and those from yellowfin muscle is in the determination of muscle mass; Altringham and Block (1997) measured wet muscle mass directly and, if there are substantial amounts of non-viable tissue in the preparations, then functional muscle mass would have been overestimated. Our estimate of isometric stress would have to be too large by a factor of 3 to account entirely for the difference (i.e. tuna red muscle could produce only 47 kN m$^{-2}$ of force, which seems unexplainably low). Altringham and Block (1997) do not report isometric stress in their study, so we cannot conclude how much of the difference can be accounted for by differences in estimates of muscle mass. Inherent differences between skipjack and yellowfin red muscle seem unlikely to be the cause of the different power outputs reported (see also below).

### *Stimulus phase and duration*

The average activation phases (EMG onset) used by swimming skipjack tuna do not change significantly with changes in tail-beat frequency (Shadwick et al., 1999; Knower et al., 1999), while the phases required to maximize work output do (Fig. 6). Thus, the phases yielding maximum work could not exactly match the phases used by swimming fish at all speeds. However, the phases used by swimming fish were not significantly different from the optimal phases at four out of six tail-beat frequencies studied and were close for the remaining two frequencies, suggesting that tuna activate their muscles very close to or at a phase that maximizes work when swimming at all speeds. Coughlin (2000) noted significant changes in the phases of red muscle activation used by trout and bass with increasing swimming speed. There were interactions in the relationship between phase, swimming speed and body position in trout (Coughlin, 2000), indicating that muscle function changed with swimming speed and body location (phases were not kept optimal for work) or that differences in contraction kinetics along the length of the animal affect optimal phase.

Similar to phase, in tuna, the optimal stimulus durations matched very closely the EMG burst durations used during swimming at both ANT and POST locations (Fig. 7). Rome and Swank (1992) noted that at warm temperatures (20 °C) the measured EMG duty cycle matched very closely that required to maximize work in scup red muscle, but that at 10 °C the measured duty cycle was much higher than optimal. Again, there is strong evidence in tuna that red muscles are being activated in a way that allows them to produce near-maximal power. Any deviation from this pattern would imply another function for the muscle.

Interestingly, we are not aware of any example of skeletal muscles involved in cyclic terrestrial locomotion that demonstrates a near-perfect match between activation parameters *in vivo* and those yielding maximum work. While muscles used to power ‘one-shot’ or ballistic types of locomotion (jumping or C-starts) are sometimes, but not always, recruited in a fashion that produces maximal power (Lutz and Rome, 1994; Olson and Marsh, 1998; Franklin and Johnston, 1997; Wakeling and Johnston, 1998), there are conceptual differences that separate these behaviours from cyclic types of locomotion. In terrestrial locomotion, it appears rare for a muscle to function solely as a power producer; requirements for support against gravity, braking and the dissipation of kinetic and gravitational potential energy during stance and limb/joint stabilization place relatively heavy ‘secondary’ demands on muscle during locomotion on land. For discussions of these competing demands and their implications for muscle function, see Biewener and Gillis (1999), Full et al. (1998) and Alexander (1997). None of these demands would be of considerable significance in thunniform locomotion, freeing the muscles to be used solely for thrust power production. Perhaps requirements to initiate, stabilize and control a propagated wave of body bending in carangiform swimmers are responsible for the submaximal power production from muscles in fish that use this mode of swimming. Thus, reports of the near-perfect match between optimal and *in vivo* activation patterns noted in this study are, not surprisingly, lacking for limb muscles used during cyclic locomotion in terrestrial vertebrates or from other fish.

It is interesting to note that muscles that power flight also appear to be used in a manner that produces large amounts of work (Biewener, 1998). Like swimming, flapping flight relies on cyclic contractions against a viscous medium to generate the required thrust and lift, with few significant ‘secondary’ demands and few mechanisms by which energy may be stored or transferred between states.

### *Effects of swimming speed on power*

In skipjack tuna, maximum power was produced by red muscle at a cycle frequency of 5 Hz (Fig. 4), the same as that reported for yellowfin tuna red muscle operating at the same temperature and similar strain (Altringham and Block, 1997). The tail-beat frequency of undisturbed yellowfin tuna averaged only 1.6 Hz at this temperature, leading Altringham and Block (1997) to suggest that a substantial reserve of red muscle power must exist in these fish most of the time. The tail-beat frequency of cruising skipjack tuna is considerably higher, probably because their smaller pectoral fins require faster swimming speeds to provide lift (Magnuson, 1978). The fish

used in our study routinely swam undisturbed in their tanks using a tail-beat frequency of 2.9±0.2 Hz ($N$=11), Knower et al. (1999) measured tail-beat frequencies of 2.8–5.2 Hz (at forced swimming speeds of 1.5–3.7 $L\,s^{-1}$) in skipjack swimming using only their red muscle, Gooding et al. (1981) reports swimming speeds requiring average tail-beat frequencies of 2.9 Hz in undisturbed skipjack tuna in a laboratory respirometer (typically ranging from 2.9 to 4.1 Hz) and Yuen (1970) estimated swimming speeds of skipjack tuna tracked in the ocean requiring tail-beat frequencies up to 3.5 Hz, and possibly faster. At the highest tail-beat frequency so measured (5.2 Hz), power output from the red muscle would be maximal, while at the lowest frequency (2.9 Hz) it would be 75–80 % maximal (Fig. 4, solid lines); at these speeds, the fish are utilizing most of the muscle's power-producing potential. These swimming speeds would not only maximize power output, but they also appear to maximize efficiency. The minimum cost of transport for 30–60 cm skipjack tuna occurs at a swimming speed of 2.1 $L\,s^{-1}$ (Gooding et al., 1981) or a tail-beat frequency of approximately 3.4 Hz.

However, while muscle that is active would be producing near-maximal power output at these speeds, it is not known whether the fish actually need to recruit all their red muscle to swim this fast. If they do, then 5 Hz would be the maximal speed at which they could swim using only red aerobic fibres. If they do not require all their red muscle at these speeds, then they could continue to increase their speed by recruiting progressively more red muscle, although the mass-specific power output would be compromised at tail-beat frequencies much higher than 5 Hz. To this end, we estimated the amount of power required to swim using oxygen consumption and compared this with the amount of red muscle required to produce that power using our measurements.

A tail-beat frequency of 3 Hz, typical of cruising skipjack tuna (see above), translates into a swimming speed of 71 $cm\,s^{-1}$ for a 43 cm (1.7 kg) tuna (Knower et al., 1999). Dewar and Graham (1994) and Boggs (1984) measured the oxygen consumed by 43–48 cm skipjack tuna (similar to the size of the fish used in the present study) as a function of swimming speed. Using an average of their measurements, a fish would require 779 $mg\,O_2\,kg^{-1}\,h^{-1}$ to swim at 71 $cm\,s^{-1}$ (i.e. with a tail-beat frequency of 3 Hz). The standard (resting) metabolic rate of a 43 cm fish is 315 $mg\,O_2\,kg^{-1}\,h^{-1}$ (Dewar and Graham, 1994). Assuming that any excess metabolism above resting values during swimming at these speeds was accounted for entirely by red muscle activity, the oxygen consumed by red muscle during swimming at 71 $cm\,s^{-1}$ is 464 $mg\,O_2\,kg^{-1}\,h^{-1}$, where kg is body mass. This assumption is not entirely valid and will overestimate the oxygen consumed by red muscle during swimming; however, the error is probably not large and, because the measurement of standard metabolic rate is from a fish in a swim-tunnel, it is also probably inflated, which will thus help counteract the overestimate of energy consumed by red muscle. Given 450 $kJ\,mol^{-1}\,O_2$ or 1 W 256 $mg^{-1}\,O_2\,h^{-1}$ of total free energy liberated from substrates and that 50 % of this can be realized as useful metabolic energy (as energy available from hydrolysis of ATP), at this swimming speed, red muscle would consume 0.91 $W\,kg^{-1}$ body mass, or 1.54 W for a 1.7 kg fish. If these aerobic muscles are 30 % efficient at converting metabolic into mechanical energy, their power output would be 0.46 W at this speed. From our calculations, red muscle produced on average 43 $W\,kg^{-1}$ at a cycle frequency of 3 Hz when activated using parameters measured from swimming fish. The red muscle mass in skipjack tuna is $0.9671M_b^{0.66}$ (Graham et al., 1983), where $M_b$ is body mass (in g), so the 0.13 kg of red muscle in a 1.7 kg skipjack can produce 5.6 W of mechanical power. Thus, the fish would have to maximally recruit 8.2 % [(0.46 W, required)/(5.6 W, available)] of its red muscle mass to swim at 71 $cm\,s^{-1}$ or with a tail-beat frequency of 3 Hz. To swim with a tail-beat frequency of 5 Hz, the highest observed in cruising skipjack, they would have to recruit approximately 50 % of their red muscle mass.

The maximum aerobic swimming speed is that at which the power required to swim equals the power available from the entire red muscle mass; for skipjack tuna, this predicts a maximum swimming speed of 4.6 $L\,s^{-1}$ or a tail-beat frequency of 5.8 Hz, which is still very close to that at which the muscles produce maximal power (Fig. 4). Thus, while the skipjack requires only 8–50 % of its red muscle mass at normal cruising speeds (tail-beat frequencies of 3–5 Hz), its maximum aerobic speed is not much faster. These fish appear to cruise at speeds close to their aerobic potential. If our estimate of isometric force and thus power, or muscle efficiency, were out by a factor of 2 in either direction, which represents a very broad scope for error, the skipjack's maximum cruising speed could require tail-beat frequencies between 4.8 and 6.5 Hz. Maximum tail-beat frequencies observed for cruising skipjack tuna of the size used in the current study are approximately 5 Hz (Knower et al., 1999; Gooding et al., 1981; Yuen, 1970), although Yuen (1970) reports following a skipjack school at sea for more than 1 h at speeds that required tail-beat frequencies in excess of 10 Hz.

The routine cruising speed of yellowfin tuna is 0.5–2 $L\,s^{-1}$ (Altringham and Block, 1997). On the basis of the energetic study of Dewar and Graham (1994) for yellowfin and the same assumptions as above, at 24 °C the red muscle of a 51 cm, 2.2 kg yellowfin tuna would consume 1.6 W of metabolic power to swim at 2 $L\,s^{-1}$ (3.2 Hz). With 30 % efficiency, the power produced by red muscle would be 0.47 W. From work loop data, it was determined that the total red muscle mass of such a fish (0.143 kg) could produce 0.5–0.7 W of power (Altringham and Block, 1997). Therefore, all the red muscle mass must be recruited to swim at these speeds, leaving the yellowfin with little scope for higher sustained aerobic speeds. Note that, because of an ambiguity in the energetic data, Altringham and Block (1997) underestimated the power required to swim by fivefold, which dramatically alters their original conclusion that yellowfin red muscle has considerable scope to power swimming at speeds above cruising (J. D. Altringham, personal commmunication). Johnson et al. (1994) also concluded that the maximum cruising speed of largemouth bass is limited by the power available from red

muscle and that, to swim faster, the fish resorts to a burst-and-glide mechanism that requires recruitment of fast white muscle, as has been suggested to occur in tuna (Johnston and Tota, 1974).

During feeding bursts at 24 °C, yellowfin tuna used tail-beat frequencies of 8–12 Hz (Altringham and Block, 1997), indicating that they must be recruiting white muscle to swim at these speeds. Peak power in yellowfin tuna red muscle occurred at approximately 5 Hz (Altringham and Block, 1997), well above the fishes' normal cruising speed of 1.6 Hz, suggesting that their red muscles are over-designed for the speeds at which they cruise, but perhaps allowing them to play a role in powering high-speed, anaerobic swimming. Maximum reported burst swimming speeds in skipjack tuna are near $20\,L\,s^{-1}$ (Magnuson, 1978), which would require tail-beat frequencies upwards of 20 Hz. The calculations above indicate that these speeds could not be powered by red muscle alone. Further, the net power output of red muscle at 20 Hz, while not measured, would be zero or, more likely, negative (Fig. 4). Thus, activation of red muscles would not contribute to, and might actually detract from, power production during sprinting at these extreme speeds. At slightly slower frequencies (13–18 Hz), the red muscle power output was around zero (Fig. 4). During high-speed burst swimming, the red muscle cannot contribute to thrust power, but it could function as a stiffening element like a tendon, perhaps to transmit some of the power generated by white muscle to the skeleton and tail. However, this hypothesis cannot be tested until it is known at what swimming speeds and tail-beat frequencies white muscle is recruited, whether red muscle continues to be activated at these high tail-beat frequencies and what the anatomical details of the white muscle/red muscle/skeletal connections are. Whether tuna white muscle produces maximal mass-specific power output at the top sprint (anaerobic) speeds is not known, but this idea has appeal because any other design would imply either carrying excess white muscle mass (i.e. operating beyond the muscle's optimal frequency for power production and thus having to recruit more muscle mass) or having muscles that are over-designed (i.e. not having enough muscle to generate the power that would allow the tail-beat frequency to reach optimal values).

Surprisingly, work output dropped substantially at slow cycle frequencies (Fig. 3). The usual observation, including in fish muscle, is for work to continue to increase with decreasing cycle frequency (e.g. Johnson and Johnston, 1991; Rome and Swank, 1992; Johnson et al., 1994). Force/velocity characteristics dictate that, as cycle frequency and shortening velocity decline, the force and thus work per cycle should increase. In skipjack red muscle, force at the onset of shortening at very slow cycle frequencies was relatively high, as expected, but the muscle could not maintain high levels of force throughout the cycle. We did not expose the muscle to equivalent stimuli during isometric contractions to determine whether the same decline in force was evident. Perhaps this decline reflects a rapid onset of fatigue. Fish are not observed to swim with such slow tail-beat frequencies, so this phenomenon probably does not affect normal swimming behaviour.

### *Twitch parameters*

The twitch kinetics of muscle fibres from the ANT and POST locations were not markedly different, although a somewhat faster onset of force and faster relaxation late in the twitch were noted in POST fibres, making those POST muscle twitches generally shorter than twitches in ANT fibres (Fig. 8). Because relaxation is very length-dependent, it is possible that the variability in relaxation rates later in the twitch is due to inconsistencies in setting the resting muscle length. As twitch rise time accounts for only one-third to one-quarter of the total twitch duration and the difference in rise time between ANT and POST locations was only 33 %, there does not appear to be a sizable difference in total twitch duration between muscle from the two locations. Indeed, the fastest ANT twitches are shorter than the slowest POST twitches. Further, as relaxation is augmented by shortening, the difference noted in relaxation late in the isometric twitch would probably be reduced during shortening contractions and thus may not play a physiologically important role during swimming. A shorter twitch rise time in POST muscle could allow a slightly later EMG onset, although the benefit of this to the animal is not immediately obvious; such a shift in EMG onset in POST muscle is not borne out in swimming fish. In any event, any differences in twitch kinetics between ANT and POST muscle fibres do not translate into significant differences in work or power potential, although POST fibres appear to be capable of maintaining power production at slightly higher cycle frequencies than those in the ANT position (Fig. 4).

The time from stimulus to peak force during isometric twitches in skipjack muscle (Fig. 8) was notably shorter than that measured in yellowfin tuna red muscle at the same temperature (approximately 90 ms in ANT and 110 ms in POST muscle) (Shadwick and Syme, 2000). However, the twitch durations of ANT red muscle in yellowfin tuna measured by Altringham and Block (1997) were not notably different from those we observed in ANT muscle of skipjack tuna: compare Fig. 8 this study with fig. 3 at 25 °C in Altringham and Block (1997). Further, while the cycle frequency at which we determined yellowfin red muscle generated maximal power (3–4 Hz) (Shadwick and Syme, 2000) was slower than that for skipjack red muscle (4–5 Hz, Fig. 4), Altringham and Block (1997) found that yellowfin red muscle generated maximal power at a cycle frequency of 5 Hz, again similar to that noted for skipjack in the current study. Thus, it is not clear whether twitch kinetics have a significant bearing on cyclic power output or the higher tail-beat frequencies seen in skipjack compared with yellowfin tuna; this relationship requires further investigation.

### *Concluding remarks*

The near-perfect match between stimulus conditions required to maximize work output in isolated muscle and those used by swimming fish is remarkable and suggests that the sole

function of all the deep red muscle in skipjack tuna is to produce maximal mechanical power to generate thrust for swimming. The shortening experienced by the muscle in swimming fish appears close to that required to maximize power, again belying its role as a power producer and perhaps reflecting the strategy of tuna of increasing tail-beat frequency rather than amplitude to increase swimming speed. The mass-specific power produced by the red muscle is maximal at the same tail-beat frequency that fish use during cruise swimming, and modelling suggests that there is not sufficient red muscle mass to power swimming at speeds much higher than these. Although mass-specific power production increases towards the posterior as a result of higher muscle strains and the relative distribution of red muscle results in an approximately 40 % higher contribution of total power from anterior regions, power output is substantial along the entire length of the body. This power is transmitted to the caudal region *via* connective tissue linkages in a near-simultaneous fashion, transmitting energy to the tail in a manner that would produce maximum thrust power. The deep red muscle of skipjack tuna can therefore be regarded as designed to produce maximum power all along the body under the conditions the fish employ during cruise swimming and so to propel the fish at speeds near the maximum of which they are capable; the fish appear to be using their red muscle to maximize swimming speed. During sprinting at frequencies near 15 Hz or greater, the red muscle, if activated, could act as a stiff element, producing no thrust power but perhaps serving to enhance the transmission of energy from white muscles to the tail, much like a tendon.

We wish to acknowledge gratefully the National Marine Fisheries Service, Keith Korsmeyer and in particular Richard Brill at the Kewalo Research Facility in Honolulu for the use of their facilities and equipment as well as their time, help and good company during these studies. Thanks to Michael Hadfield for the use of video equipment used to photograph swimming tunas. This research was supported by the National Science Foundation (IBN95-14203 and IBN00-91987) (R.E.S.) and the Natural Science and Engineering Research Council of Canada (D.A.S.).

## References

**Alexander, R. McN.** (1997). Optimum muscle design for oscillatory movements. *J. Theor. Biol.* **184**, 253–259.

**Altringham, J. D. and Block, B. A.** (1997). Why do tuna maintain elevated slow muscle temperatures? Power output of muscle isolated from endothermic and ectothermic fish. *J. Exp. Biol.* **200**, 2617–2627.

**Altringham, J. D. and Ellerby, D. J.** (1999). Fish swimming patterns in muscle function. *J. Exp. Biol.* **202**, 3397–3403.

**Altringham, J. D. and Johnston, I. A.** (1988). The mechanical properties of polyneuronally innervated, myotomal muscle fibres isolated from a teleost fish (*Myoxocephalus scorpius*). *Pflügers Arch.* **412**, 524–529.

**Altringham, J. D., Wardle, C. S. and Smith, C. I.** (1993). Myotomal muscle function at different points on the body of a swimming fish. *J. Exp. Biol.* **182**, 191–206.

**Biewener, A. A.** (1998). Muscle function *in vivo*; a comparison of muscles used for elastic energy savings *versus* muscles used to generate mechanical power. *Am. Zool.* **38**, 703–717.

**Biewener, A. A. and Gillis, G. B.** (1999). Dynamics of muscle function during locomotion: accommodating variable conditions. *J. Exp. Biol.* **202**, 3387–3396.

**Biewener, A. A., Konieczynski, D. D. and Baudinette, R. V.** (1998). *In vivo* muscle force–length behavior during steady-speed hopping in tammar wallabies. *J. Exp. Biol.* **201**, 1681–1694.

**Boggs, C. H.** (1984). Tuna bioenergetics and hydrodynamics. PhD dissertation, University of Wisconsin, Madison, USA.

**Bottinelli, R., Schiaffino, S. and Reggiani, C.** (1991). Force–velocity relations and myosin heavy chain isoform compositions of skinned fibres from rat skeletal muscle. *J. Physiol., Lond.* **437**, 655–672.

**Close, R. I.** (1972). Dynamic properties of mammalian skeletal muscles. *Physiol. Rev.* **52**, 129–197.

**Coughlin, D. J.** (2000). Power production during steady swimming in largemouth bass and rainbow trout. *J. Exp. Biol.* **203**, 617–629.

**Davies, M. and Johnston, I. A.** (1993). Muscle fibres in rostral and caudal myotomes of the Atlantic cod have different contractile properties. *J. Physiol., Lond.* **459**, 8P.

**Dewar, H. and Graham, J. B.** (1994). Studies of tropical tuna swimming performance in a large water tunnel. I. Energetics. *J. Exp. Biol.* **192**, 13–31.

**Eddinger, T. J.** (1998). Myosin heavy chain isoforms and dynamic contractile properties: skeletal *versus* smooth muscle. *Comp. Biochem. Physiol.* **119B**, 425–434.

**Ellerby, D. J., Altringham, J. D., Williams, T. and Block, B. A.** (2000). Slow muscle function of Pacific bonito (*Sarda chiliensis*) during steady swimming. *J. Exp. Biol.* **203**, 2001–2013.

**Franklin, C. E. and Johnston, I. A.** (1997). Muscle power output during escape responses in an Antarctic fish. *J. Exp. Biol.* **200**, 703–712.

**Full, R. J., Stokes, D. R., Ahn, A. N. and Josephson, R. K.** (1998). Energy absorption during running by leg muscles in a cockroach. *J. Exp. Biol.* **201**, 997–1012.

**George, J. C. and Stevens, E. D.** (1978). Fine structure and metabolic adaptation of red and white muscles in tuna. *Env. Biol. Fish.* **3**, 185–191.

**Gooding, R. M., Neill, W. H. and Dizon, A. E.** (1981). Respiration rates and low oxygen tolerance limits in skipjack tuna, *Katsuwonus pelamis*. *Fish. Bull. Fish Wildl. Serv. US* **79**, 31–48.

**Graham, J. B., Koehrn, F. J. and Dickson, K. A.** (1983). Distribution and relative proportions of red muscle in scombrid fishes: consequences of body size and relationships to locomotion and endothermy. *Can. J. Zool.* **61**, 2087–2096.

**Hammond, L., Altringham, J. D. and Wardle, C. S.** (1998). Myotomal slow muscle function of rainbow trout *Oncorhynchus mykiss* during steady swimming. *J. Exp. Biol.* **201**, 1659–1671.

**Johnson, T. P. and Johnston, I. A.** (1991). Power output of fish muscle fibres performing oscillatory work: effects of acute and seasonal temperature change. *J. Exp. Biol.* **157**, 409–423.

**Johnson, T. P., Syme, D. A., Jayne, B. C., Lauder, G. V. and Bennett, A. F.** (1994). Modeling red muscle power output during steady and unsteady swimming in largemouth bass. *Am. J. Physiol.* **267**, R481–488.

**Johnston, I. A. and Tota, B.** (1974). Myofibrillar ATPase in the various red and white trunk muscles in the tunny (*Thunnus thynnus* L.) and the tub gurnard (*Trigla lucerna* L.). *Comp. Biochem. Physiol.* **49B**, 367–373.

**Joseph, J., Klawe, W. and Murphy, P.** (1988). *Tuna and Billfish – Fish Without a Country.* La Jolla: Inter-American Tropical Tuna Commission.

**Josephson, R. K.** (1985). Mechanical power output from striated muscle during cyclic contraction. *J. Exp. Biol.* **114**, 493–512.

**Josephson, R. K.** (1993). Contraction dynamics and power output of skeletal muscle. *Annu. Rev. Physiol.* **55**, 527–546.

**Katz, S. L., Syme, D. A. and Shadwick, R. E.** (2001). High speed swimming: enhanced power in yellowfin tuna. *Nature* **410**, 770–771.

**Knower, T., Shadwick, R. E., Katz, S. L., Graham, J. B. and Wardle, C. S.** (1999). Red muscle activation patterns in yellowfin (*Thunnus albacares*) and skipjack (*Katsuwonus pelamis*) tunas during steady swimming. *J. Exp. Biol.* **202**, 2127–2138.

**Langfeld, K. S., Altringham, J. D. and Johnston, I. A.** (1989). Temperature and the force–velocity relationship of live muscle fibres from the teleost *Myoxocephalus scorpius*. *J. Exp. Biol.* **144**, 437–448.

**Lutz, G. J. and Rome, L. C.** (1994). Built for jumping: the design of the frog muscular system. *Science* **263**, 370–372.

**Magnuson, J. J.** (1978). Locomotion by scombrid fishes: Hydromechanics, morphology and behavior. In *Fish Physiology*, vol. VII (ed. W. S. Hoar and D. J. Randall), pp. 240–315. New York: Academic Press.

**Mathieu-Costello, O., Agey, P. J., Logemann, R. B., Brill, R. W. and**

**Hochachka, P. W.** (1992). Capillary–fiber geometrical relationships in tuna red muscle. *Can. J. Zool.* **70**, 1218–1229.

**Olson, J. M. and Marsh, R. L.** (1998). Activation patterns and length changes in hindlimb muscles of the bullfrog *Rana catesbeiana* during jumping. *J. Exp. Biol.* **201**, 2763–2777.

**Rayner, M. D. and Keenan, M. J.** (1967). Role of red and white muscles in the swimming of the skipjack tuna. *Nature* **214**, 392–393.

**Roberts, T. J., Marsh, R. L., Weyand, P. G. and Taylor, C. R.** (1997). Muscular force in running turkeys: the economy of minimizing work. *Science* **275**, 1113–1115.

**Rome, L. C. and Sosnicki, A. A.** (1990). The influence of temperature on mechanics of red muscle in carp. *J. Physiol., Lond.* **427**, 151–169.

**Rome, L. C., Sosnicki, A. and Choi, I.** (1992). The influence of temperature on muscle function in the fast-swimming scup. II. The mechanics of red muscle. *J. Exp. Biol.* **163**, 281–295.

**Rome, L. C. and Swank, D.** (1992). The influence of temperature on power output of scup red muscle during cyclical length changes. *J. Exp. Biol.* **171**, 261–281.

**Rome, L. C., Swank, D. and Corda, D.** (1993). How fish power swimming. *Science* **261**, 340–343.

**Shadwick, R. E., Katz, S. L., Korsmeyer, K. E., Knower, T. and Covell, J. W.** (1999). Muscle dynamics in skipjack tuna: timing of red muscle shortening in relation to activation and body curvature during steady swimming. *J. Exp. Biol.* **202**, 2139–2150.

**Shadwick, R. E., Steffensen, J. F., Katz, S. L. and Knower, T.** (1998). Muscle dynamics in fish during steady swimming. *Am. Zool.* **38**, 755–770.

**Shadwick, R. E. and Syme, D. A.** (2000). Mechanical power production by red and white swimming muscles of yellowfin tuna (*Thunnus albacares*). *Am. Zool.* **40**, 1208.

**Sieck, G. C., Han, Y., Prakash, Y. S. and Jones, K. A.** (1998). Cross-bridge cycling kinetics, actomyosin ATPase activity and myosin heavy chain isoforms in skeletal and smooth respiratory muscles. *Comp. Biochem. Physiol.* **119B**, 435–450.

**Stevenson, R. D. and Josephson, R. K.** (1990). Effects of operating frequency and temperature on mechanical power output from moth flight muscles. *J. Exp. Biol.* **149**, 61–78.

**Wakeling, J. M. and Johnston, I. A.** (1998). Muscle power output limits fast-start performance in fish. *J. Exp. Biol.* **201**, 1505–1526.

**Wardle, C. S., Videler, J. J. and Altringham, J. D.** (1995). Tuning in to fish swimming waves: body form, swimming mode and muscle function. *J. Exp. Biol.* **198**, 1629–1636.

**Wardle, C. S., Videler, J. J., Arimoto, T., Franco, J. M. and He, P.** (1989). The muscle twitch and the maximum swimming speed of giant bluefin tuna, *Thunnus thynnus*. *J. Fish Biol.* **35**, 129–137.

**Westneat, M. W., Hoese, W., Pell, C. A. and Wainwright, S. A.** (1993). The horizontal septum: mechanisms of force transfer in locomotion of scombrid fishes (Scombridae, Perciformes). *J. Morphol.* **217**, 183–204.

**Yuen, H. S. H.** (1970). Behavior of skipjack tuna, *Katsuwonus pelamis*, as determined by tracking with ultrasound devices. *J. Fish. Res. Bd. Can.* **27**, 2071–2079.

**Zhang, G. X., Swank, D. M. and Rome, L. C.** (1996). Quantitative distribution of muscle fiber types in the scup *Stenotomus chrysops*. *J. Morphol.* **229**, 71–81.